Fermi National Accelerator Laboratory

FERMILAB-Pub-91/164-A
June 1991

# Aspects of Reheating in First-Order Inflation

Richard Watkins

Department of Astronomy and Astrophysics
Enrico Fermi Institute
The University of Chicago
Chicago, IL 60637 U.S.A.

NASA/Fermilab Astrophysics Center
Fermi National Accelerator Laboratory
P.O. Box 500, Batavia, IL 60510 U.S.A.

Lawrence M. Widrow

Canadian Institute for Theoretical Astrophysics
University of Toronto
60 St. George Street
Toronto, ON M5S 1A1 Canada

**Abstract**

We study reheating in theories where inflation is completed by a first-order phase transition. In these scenarios, the Universe decays from its false vacuum state by bubble nucleation. In the first stage of reheating, vacuum energy is converted into kinetic energy for the bubble walls. To help understand this phase we derive a simple expression for the equation of state of a universe filled with expanding bubbles. Eventually, the bubble walls collide. We present numerical simulations of two-bubble collisions clarifying and extending previous work by Hawking, Moss, and Stewart. Our results indicate that wall energy is efficiently converted into coherent scalar waves. We go on to discuss particle production due to quantum effects. These effects lead to the decay of the coherent scalar waves. In addition, they lead to direct particle production during bubble-wall collisions. We calculate particle production for colliding walls in both sine-Gordon and $\phi^4$ theories and show that it is far more efficient in the $\phi^4$ case. The relevance of our work for recently proposed models of first-order inflation is discussed.

Operated by Universities Research Association Inc. under contract with the United States Department of Energy

## 1. Introduction

In Guth's original version of inflation [1], the Universe decays from its initial false-vacuum state by the nucleation of true-vacuum bubbles. As the bubbles expand, the energy in the false vacuum is converted into kinetic energy for the bubble walls. In theory, the walls eventually collide, the true vacuum percolates, and wall energy is converted into radiation, reheating the Universe. Unfortunately, in Guth's model the nucleation and expansion of bubbles cannot keep up with the exponential expansion of the regions still trapped in the false vacuum, and the true vacuum never percolates [2]. This is known in the literature as the 'graceful exit' problem.

Clearly, first-order inflation (generically, any model in which inflation is completed by a strongly first-order phase transition) can work if either the nucleation or expansion rate changes during the inflationary phase. For example, in the extended inflation scenario proposed by La and Steinhardt [3] the Hubble parameter in the vacuum-energy dominated ($p = -\rho$) Universe decreases with time, thus enabling the true vacuum to percolate. While La and Steinhardt's proposal suffered a graceful exit problem of its own [4], there has been no shortage of theories which purport to save the general idea of first-order inflation [5].

Given the renewed interest in first-order inflation, we felt it an opportune time to examine some of the nuts and bolts of reheating in these models. Reheating in new [6] and chaotic [7] inflation has been examined in some detail [8]. The analysis in these scenarios is simplified by the fact that the Universe can be treated as homogeneous (Friedmann-Robertson-Walker) throughout. Inflation occurs when some order parameter or scalar field finds itself displaced from the minimum of its potential. At first, the field slowly rolls towards this minimum. During this phase the energy density $\rho$ of the Universe is dominated by vacuum energy with $\rho = \text{const}' \equiv \rho_{vac}$; the pressure $p = -\rho$; and the scale factor $a \propto e^{H_I t}$, where $H_I^2 = 8\pi\rho_{vac}/3m_{pl}^2$. (We use units where $\hbar = c = k_B = 1$ and $m_{pl} = G_{\text{Newton}}^{-1/2} \simeq 10^{19}\text{GeV}$ is the Planck mass). As the inflaton reaches the minimum, the slope of the potential increases and the field begins to oscillate about the minimum on a time scale short compared to the Hubble time. These oscillations behave at first like pressureless nonrelativistic matter so that $a \propto t^{2/3}$. Eventually, the oscillations decay into relativistic particles and the Universe becomes radiation-dominated. We note that if the lifetime of the inflaton is long compared to $H_I^{-1}$, most of the energy in the $\phi$ field will be diluted by cosmological expansion and the reheat temperature $T_{RH}$ ( $\sim (m_{pl}\Gamma_\phi)^{1/2}$) will be well below $\rho_{vac}^{1/4}$, the energy scale associated with the false vacuum.

The physics of reheating in first-order inflation is essentially the same as in new and chaotic inflation: Energy initially stored in a coherent scalar field must be converted into radiation. However, the situation is considerably more difficult to analyze. Here, both the field $\phi$ and the metric are inhomogeneous. Furthermore, reheating involves a mix of quantum physics (bubble nucleation and particle creation) and classical physics (expansion and collisions of bubbles). Difficulties aside, a number of authors have focused on the potentially rich phenomenology associated with these scenarios. For example, it has been suggested that gravitational waves [9], black holes [10][11], topological defects [12], and the baryon asymmetry [13][11] may have been produced during the phase transition. Whether or not such phenomena actually occur depends in part on the details of reheating. For

example, in the baryogenesis scenario of Ref.[13] it is important to know the spectrum of particles produced in wall collisions.

This work represents a modest attempt at understanding the mechanics of reheating in first-order inflation. Reheating in these models involves three processes: bubble expansion; bubble collisions; and particle production. As discussed above, bubble expansion is the process whereby the energy stored in the (false) vacuum is converted into kinetic energy of the bubble walls. During this time, $p/\rho$ increases from its initial value of $-1$. In Section 3 we derive a simple expression for the equation of state of a universe dominated by bubbles which are expanding but have not yet collided. In Section 4 we consider the classical evolution of colliding bubbles and focus on the production of classical scalar waves. This is the dominant process for converting wall energy into a form that can decay into radiation and is therefore a crucial intermediate step in the reheating process. Our results indicate that wall energy is efficiently converted into scalar waves, though it is fair to say that we have not explored the entire range of bubble parameters. If indeed scalar waves are efficiently produced, then reheating will occur much as it does in new and chaotic inflation, and the reheat temperature will be set by the decay width of the inflaton. Alternatively, if this is not the case, scalar dynamics will play the dominant role in determining the reheat temperature. In Section 5 we show how to calculate the quantum particle production rate from classical scalar field configurations. We apply our methods to the case of interacting domain walls and determine the number of particles produced during a collision. We focus on the difference between walls which arise in $\phi^4$ theories and those which arise in sine-Gordon (SG) theories and show that, at least for relativistic walls, particle production is far more efficient in the $\phi^4$ case. Section 6 presents some conclusions and a discussion of the relevance our work has for first-order inflation scenarios.

## 2. Preliminaries

In a first-order phase transition, the Universe decays from a metastable state by bubble nucleation. A nucleated bubble is essentially a true vacuum fluctuation that is large enough to grow classically. In inflation the phase transition occurs at essentially zero temperature, and bubble nucleation takes place through quantum fluctuations.

The nucleation rate is determined by considering the most likely fluctuation that is able to grow. Coleman [14] (see also Ref.[15]) has shown that this most likely fluctuation is a spherical bubble nucleated at rest with a certain critical size determined by microphysics. Coleman's method will be discussed in Section 4. Here we review some basic properties of 'critical' bubbles in an expanding universe. Consider the theory of a real scalar field $\phi$ described by the Lagrangian

$$\mathcal{L} = \frac{1}{2}\partial_\mu\phi\partial^\mu\phi - V(\phi) \tag{2.1}$$

where $V(\phi)$ has two nondegenerate minima. For definiteness, we take the potential to be

$$V(\phi) = \frac{\lambda}{8}\left(\phi^2 - \phi_o^2\right)^2 + \epsilon\phi_o^3\left(\phi + \phi_o\right) \tag{2.2}$$

though any asymmetric double-well potential will do. We shall generically refer to models of this type as $\phi^4$ models. Focus for the moment on the case where $\epsilon \ll \lambda$ so that the energy difference between true and false minima is small compared to the height of the barrier. To lowest order in $\epsilon$, the true and false minima are at $-\phi_o$ and $\phi_o$ respectively. The mass of $\phi$-excitations in either of these minima is given by $m_\phi = \lambda^{1/2}\phi_o$, and $\rho_{vac} = 2\epsilon\phi_o^4$. $\epsilon \ll \lambda$ corresponds to the thin-wall limit in which the radius of the bubbles is much greater than the thickness of the wall separating the interior true vacuum region from the exterior false vacuum region. One nice feature of the thin-wall limit is that the properties of individual bubbles can be determined analytically. In particular, the thickness of the bubble wall is $\Delta = 2/\left(\lambda^{1/2}\phi_o\right) = 2m_\phi^{-1}$, the surface energy density is $\sigma = 2\lambda^{1/2}\phi_o^3/3$, and the radius of the bubble at the time of nucleation is $R_o = \lambda^{1/2}/\left(\epsilon\phi_o\right) = 3\sigma/\rho_{vac}$. $R_o/\Delta \simeq \lambda/\epsilon \gg 1$ so the bubble walls are indeed thin.

The results quoted above are valid so long as gravity is not important. Gravity becomes important when the radius of the bubbles becomes comparable to the Hubble radius [16]. For the case at hand, the Hubble radius is given by $H^{-1} = \left[8\pi\rho_{vac}/3m_{pl}^2\right]^{-1/2} \simeq m_{pl}/\left(\epsilon^{1/2}\phi_o^2\right)$. $RH \simeq \left(\lambda/\epsilon\right)^{1/2}\phi_o/m_{pl}$ is therefore a measure of how important gravity is.

The nucleation rate per unit volume (number of bubbles nucleated per unit four-volume) is [17]

$$\Gamma \simeq A\left(m_\phi\right)^4 e^{-S_E} \tag{2.3}$$

where $A$ is a constant of order unity and $S_E$ is the Euclidean action for the bounce solution corresponding to a critical bubble. For the thin wall case, $S_E = \pi^2\lambda^2/3\epsilon^3$. Perhaps the most important parameter describing a first-order inflation theory is $\eta \equiv \Gamma/H^4$, the so-called percolation parameter. $\eta$ gives roughly the number of bubbles nucleated per horizon volume per Hubble time. For the case at hand

$$\eta \simeq \left(\frac{\lambda}{\epsilon}\right)^2 \left(\frac{m_{pl}}{\phi_o}\right)^4 e^{-\pi^2\lambda^2/3\epsilon^3} \ . \tag{2.4}$$

The requirement that inflation last long enough to solve the horizon and flatness problems constrains $\eta$ to be less than about $10^{-3}$, whereas percolation of the true vacuum bubbles can only occur if $\eta > O(0.1)$. In Guth's model, $\eta$ is constant and the model is untenable. In the models of Ref.[5] , $\eta$ varies in time; a period of inflation with $\eta < 10^{-3}$ precedes the percolation phase in which $\eta$ is large.

The mean separation between bubbles is roughly $D \simeq \Gamma^{-1/4} = \eta^{-1/4}H^{-1} \simeq \left(\lambda^{1/2}\phi_o\right)^{-1} e^{S_E/4}$. Certainly, a key unknown is the value (or range of values) $\eta$ has when percolation occurs. (Remember that $\eta$ is increasing with time.) For $\eta \gg 1$, $D$ will be less than the Hubble radius and there will be many bubbles within a given Hubble volume. In this case, cosmological expansion can be neglected in treating the dynamics of the bubbles. On the other hand, if $\eta \sim 1$ when percolation occurs, $D$ will be of order the horizon and cosmological expansion will play an essential role in the bubble dynamics. In what follows we will neglect, for the most part, cosmological expansion in treating the bubbles, but only because it simplifies the calculations. We leave the full problem of bubble dynamics in an expanding spacetime for future investigations.

As we will see, the ratio $R_o/D$ is also essential in describing the phase transition. Once a bubble is nucleated it begins to expand, and the velocity of the walls rapidly approaches the speed of light. The surface energy density and thickness of a wall depend on its velocity $\dot{R} \equiv dR/dt$, or equivalently on the relativistic Lorentz factor $\gamma = 1/\sqrt{1-\dot{R}^2}$; the energy density grows like $\gamma$ and the thickness decreases like $\gamma^{-1}$. These properties determine to a large degree the masses and quantities of particles produced in a collision between walls. For subhorizon-sized bubbles, $\gamma = R(t)/R_o$ [14] . The quantity $D/R_o$ therefore tells us how relativistic the walls are before they collide. In our example, $D/R_o = (\epsilon/\lambda)\, e^{\pi^2\lambda^2/12\epsilon^3}$.

## 3. Expanding Bubbles

During reheating the equation of state of the Universe changes from $p = -\rho$ (vacuum dominated) to $p = \rho/3$ (radiation dominated). The first step in this process is the nucleation and expansion of bubbles during which vacuum energy is converted into kinetic energy for the walls.

We can be a bit more quantitative by considering an idealized model of a universe filled with bubbles that are expanding but have not yet collided. Let us assume $R_o < D \ll H^{-1}$, so that self-gravity and cosmological expansion effects on the evolution of the bubbles can be neglected. In addition, we assume that all of the bubbles are nucleated simultaneously. In principle, each of these assumptions can be relaxed; we believe, however, that the simplified case considered here adequately illustrates the physics we are interested in. We now derive the equation of state for our idealized universe (A similar analysis for a general domain wall network was carried out in [18]). This is done by calculating the average energy and pressure densities for a sphere of radius $D$ centered about a single bubble of radius $R(t)$. In particular, we calculate

$$\begin{aligned} \bar{\rho} &= \Omega^{-1} \int d^3x T^{00} \\ \bar{p} &= -\Omega^{-1} \int d^3x T^{ii} \end{aligned} \tag{3.1}$$

where $\Omega \equiv 4\pi D^3/3$, $T^{\mu\nu}$ is the stress energy for the inflaton field, and $i = 1, 2, 3$.

We consider the contributions to the average energy and pressure densities from the false vacuum region outside the bubble and the bubble wall separately. For the contribution from the false vacuum we find

$$\begin{aligned} \bar{\rho}_{\text{false vacuum}} &= \rho_{vac}\left(1 - \frac{R^3}{D^3}\right) \\ \bar{p}_{\text{false vacuum}} &= -\bar{\rho}_{\text{false vacuum}} \,. \end{aligned} \tag{3.2}$$

We treat the bubble wall as an infinitesimally thin shell of stress-energy and use the Gauss-Codazzi formalism as developed by Israel [19]. Let $\xi^a$ be the unit spacelike normal to the wall hypersurface. For an expanding bubble $\xi^a = \left(\gamma\dot{R},\ \gamma\sin\theta\cos\varphi,\ \gamma\sin\theta\sin\varphi,\ \gamma\cos\theta\right)$.

Let $T^W_{ab}$ be the stress energy for the wall. In the thin wall approximation $T^W_{ab}$ has a $\delta$-function singularity across the wall. It is convenient to define the quantity

$$S_{ab} \equiv \int dl\, T^W_{ab} \tag{3.3}$$

where $l$ is the proper distance through the surface in the direction of $\xi_a$. We note that $dl = \gamma dr$.

The three metric intrinsic to the wall is

$$h_{ab} = g_{ab} - \xi_a \xi_b \ . \tag{3.4}$$

For domain walls, $S_{ab} = -\sigma h_{ab}$. In addition bubbles nucleated by quantum tunneling have $3\sigma/R_o = \rho_{vac}$. It is straightfoward to show that

$$\begin{aligned} \Omega^{-1} \int d^3x T^W_{00} &= \frac{3\gamma\sigma R^2}{D^3} \\ &= \rho_{vac} \frac{R^3}{D^3} \\ \Omega^{-1} \int d^3x T^W_{ii} &= \rho_{vac} \frac{R^3}{D^3} \left( \frac{1}{\gamma^2} - \frac{1}{3} \right) \ . \end{aligned} \tag{3.5}$$

Combining Eq.(3.2) and Eq.(3.5) we find

$$\begin{aligned} \bar{\rho} &= \rho_{vac} \\ \bar{p} &= -\rho_{vac} \left( 1 + \left( \frac{R}{D} \right)^3 \left( \frac{4}{3} - \frac{1}{\gamma^2} \right) \right) \ . \end{aligned} \tag{3.6}$$

For $R \ll D$, $\bar{p} \simeq -\rho_{vac}$ as expected; the Universe in this case is essentially dominated by vacuum energy. If, on the other hand, bubbles are nucleated with $R_o \simeq D$, then $\bar{p} = -2\bar{\rho}/3$ right after nucleation. This is just the equation of state for a wall-dominated Universe. In fact, the Universe is still undergoing power-law inflation when the bubbles first collide [20]. Finally, if $R_o \ll D$, the walls will be relativistic by the time they collide, and the equation of state just before bubble collisions will be $\bar{p} = \bar{\rho}/3$.

## 4. Bubble Collisions: Classical Treatment

Bubble collisions provide the next step in reheating. Collisions release energy bound in the walls through both quantum and classical processes. Quantum effects will be discussed in Section 5. Here, we treat the bubble walls as classical field configurations and show that classical scalar waves are emitted during a collision. We explore this process by studying the collision of two expanding bubbles.

The two-bubble problem was studied by Hawking, Moss, and Stewart (HMS). Here, we elucidate their results and extend the analysis to include discussion relevant to the problem at hand. HMS considered theories in which the true vacuum manifold consists of a degenerate family of local minima. In particular, they considered a scalar-Yang-Mills gauge theory in which the true vacuum manifold is a circle of radius $v$, so that inside a given bubble $\phi = ve^{i\alpha}$. HMS followed the collision of two bubbles, focusing on the case where the phase $\alpha$ differs from one bubble to the next. They showed that energy in the bubble walls is released in the form of phase waves, and that the amount of radiation depends on the difference in $\alpha$ from one bubble to the next. Here we consider the simpler theory of a real scalar field with a nondegenerate vacuum. As we will see, energy is released in the form of coherent scalar waves. Evidently, the complexity of the HMS model is unnecessary for reheating.

It is important to bear in mind that two-bubble (or few-bubble for that matter) collisions are inefficient at producing large thermalized regions [2]. Reheating in first-order inflation is necessarily a many-bubble process. However, we can learn much from two-bubble collisions that is relevant for the general problem.

The initial configuration and subsequent evolution of the scalar field for the two-bubble problem discussed here is rather special and depends on the physics of bubble nucleation in the context of false vacuum decay. We therefore take some time to review the basics of vacuum decay. Coleman [14] has developed a simple technique for calculating the bubble nucleation rate in flat space and at zero temperature based on the Euclidean path integral formulation of scalar field theory. He finds that the nucleation rate is proportional to $e^{-S_E}$, where $S_E$ is the Euclidean action for a solution to the Euclidean equations of motion. Because of the exponential dependence on $S_E$, we are only interested in the solution of least action, which in flat space is the $O(4)$ symmetric 'bounce' solution. The field configuration of a critical bubble (discussed above) is just the $\tau = 0$ slice of the 'bounce' solution.

The evolution of an expanding bubble can be determined in one of two ways. First, we can take the field configuration of a critical bubble as initial data and evolve this configuration forward in time. A simpler and more elegant approach takes advantage of the high degree of symmetry in the problem. As noted by Coleman, the Lorentzian equations of motion are just the analytic continuation of the Euclidean equations, and the real time evolution of a bubble is given by the analytic continuation of the Euclidean bounce solution. The $O(4)$ symmetry in Euclidean space carries over to an $O(3,1)$ symmetry in Minkowski space.

Proper use of the $O(3,1)$ symmetry requires two coordinate systems to cover all of Minkowski space. For $|\vec{r}| > |t|$ (Region I) we choose the coordinates $(\rho, \psi, \theta, \varphi)$ where

$$\begin{aligned} x &= \rho \cosh\psi \sin\theta \cos\varphi \qquad & z &= \rho \cosh\psi \cos\theta \\ y &= \rho \cosh\psi \sin\theta \sin\varphi \qquad & t &= \rho \sinh\psi \ . \end{aligned} \tag{4.1}$$

In these coordinates, and with the assumption of $O(3,1)$ symmetry, the equations of motion are identical to those in Euclidean space with $O(4)$ symmetry, and the Euclidean bounce solution gives the field configuration for an expanding bubble.

For $|r| < |t|$ (Region II), we require a different coordinate system $(\rho', \psi', \theta, \varphi)$ with

$$\begin{aligned} x &= \rho' \sinh\psi' \sin\theta \cos\varphi \qquad & z &= \rho' \sinh\psi' \cos\theta \\ y &= \rho' \sinh\psi' \sin\theta \sin\varphi \qquad & t &= \rho' \cosh\psi' \ . \end{aligned} \tag{4.2}$$

In order to find the field configuration in this region one needs to take the field configuration on the $\rho = 0$ hypersurface (from the Region I solution) and evolve into Region II. Since the field configuration only depends on $\rho$ this amounts to solving an ordinary differential equation. For a single thin-wall bubble, the bubble wall is entirely in Region I. The field is essentially constant in Region II, so that evolving the field is usually unnecessary.

The situation changes with more than one bubble. Consider the nucleation of two bubbles. In general this is a complicated process and one that has yet to be treated in the literature. If, however, the bubbles are widely separated at the time of nucleation, then they can be treated as noninteracting (the dilute instanton approximation), and the generalization from the single bounce solution is straightfoward. For two bubbles, the axis joining their centers will be a preferred direction, so that the solution to the Euclidean equations of motion for noninteracting bubbles will have $O(3)$ symmetry. We consider first a coordinate system in which the $\tau = 0$ hypersurface intersects the centers of the two bubbles. The field configuration on this hypersurface becomes initial data for two simultaneously nucleated expanding bubbles in Minkowski space, and one could solve for the field configurations numerically by solving the classical equations of motion. As in the single bubble case, a more efficient technique for finding the evolution exploits the extra boost symmetry of the problem. Here the $O(3)$ symmetry of the two-bubble Euclidean bounce translates to an $O(2,1)$ symmetry in Minkowski space. Let the $z$-axis correspond to the the line connecting the centers of the bubbles. As before, spacetime is divided into two regions. For $|t| < \sqrt{x^2 + y^2}$ we choose the coordinates $(s, \psi, \theta, z)$ with

$$\begin{aligned} x &= s \cosh\psi \sin\theta \qquad & z &= z \\ y &= s \cosh\psi \cos\theta \qquad & t &= s \sinh\psi \ . \end{aligned} \tag{4.3}$$

The solution in this region of spacetime is given by the analytic continuation of the two bubble bounce solution. For $|t| > \sqrt{x^2 + y^2}$ we take

$$\begin{aligned} x &= s' \sinh\psi' \sin\theta \qquad & z &= z \\ y &= s' \sinh\psi' \cos\theta \qquad & t &= s' \cosh\psi' \ . \end{aligned} \tag{4.4}$$

To find the field configuration in this region, we take the solution on the $t = r \equiv \sqrt{x^2 + y^2}$ hypersurface and solve the equations of motion. Here the equations we are required to solve are $1 + 1$ ($s$ and $z$) partial differential equations. For the two bubble case, all of the interaction between the bubbles takes place in this second region.

The procedure outlined above was developed and used by HMS. Here we consider bubbles in a theory described by Eqs.(2.1,2.2) with $\epsilon = 0.1$. In Fig. 1a, we show the field $\phi(s, z)$ in the collision region for two simultaneously nucleated bubbles. In Fig. 1b, the

separation between the bubbles has been doubled. The figures illustrate that the general behavior of the field scales with $D$ and is roughly independent of $R_o$ and $\Delta$. This result holds so long as $D \gg (R_o,\ \Delta)$.

It is useful to view the collision in physical coordinates. For example, Fig. 1 also gives the $r = 0,\ t - z$ spacetime diagram. Fig. 2 shows the collision in the $t - r$ plane for fixed $z$, while snapshots at different times are shown in Fig. 3. An observer near $z = 0$ will alternate between false and true vacua. Observers at different values of $r$ will see the same sequence of events but at different times. For example, if an observer at $r = 0$ sees the false vacuum change to true at $t = t_0$ then an observer at $r = r_1$ will see false change to true at a time $t_1 = \sqrt{t_0^2 + r_1^2}$.

The results described above also give the field configuration for a big bubble colliding with a small bubble. Because of the $O(2,1)$ symmetry, an observer Lorentz-boosted in either the $x$ or $y$ directions will see the same field configuration as given above. However, to an observer moving in the $z$ direction one bubble will appear to be nucleated before the other. In this frame, the bubble which is nucleated first will be larger at the time of the collision. The field configurations in the two frames are related by a Lorentz transformation.

Let us be a bit more quantitative. Consider two bubbles, nucleated about the spacetime events $t = x = y = z = 0$ and $t = t_o,\ z = z_o,\ x = y = 0$, where $z_o > t_o$. The two bubbles will first collide at $z_c = \left(z_o + t_o\sqrt{1 - R_o^2/\left(z_o^2 - t_o^2\right)}\right)/2,\ x = y = 0$ and $t_c = \sqrt{z_c^2 - R_o^2}$. The ratio of the bubble radii when they first collide is $z_c/\left(z_o - z_c\right)$. For $R_o^2 \gg z_o^2 - t_o^2$, this is just $\left(z_o + t_o\right)/\left(z_o - t_o\right)$. A Lorentz transformation with $v_o = t_o/z_o$ will give us the field configuration for two equal sized bubbles separated by a distance $2D = z_o/\gamma$. Now consider the radiation that is produced during the collision. In the equal-bubble frame, the radiation is symmetric about $z = 0$ and moves outward from the collision region. Suppose that in the equal-bubble frame, a scalar wave has a $z$-component of velocity $v_z$ (recall that these are massive excitations). In the Lorentz-boosted frame, it will have velocity $v_z' = \left(v_o + v_z\right)/\left(1 + v_z v_o\right)$. Clearly, a wave with $|v_z| < |v_o|$ will be moving away from the center of the large bubble when viewed in the Lorentz-boosted frame. A schematic of this situation is shown in Fig. 4.

Weinberg [4] has pointed out that bubbles nucleated early in the epoch of inflation are too large by the end of inflation to thermalize. The discussion here illustrates that thermalization of big bubbles by collisions with smaller bubbles may be more difficult than expected, since much of the radiation released in the collision may continue to move outward from the center of the large bubble. Ultimately, this issue will have to be resolved by numerical simulation.

As noted by HMS (and evidenced in the figures) when two domain walls collide they do not immediately annihilate into a burst of radiation. Rather, the two walls reflect off of one another and are then drawn back together by the false vacuum pressure for another collision. In general, each collision releases some fraction of the walls' energy into scalar waves, and all of the energy is eventually radiated away. In the example shown in the figures, most of the energy is radiated away in a time interval $\tau_0 \equiv t_f - t_i = O(D)$, where $t_i$ is the time when the walls first collide and $t_f$ is the point where most of the energy has been dissipated. Here $t_f$ and $t_i$ are defined for an observer at the origin. For

an observer at $z = 0$ but arbitrary $r$, $\tau(r) = \sqrt{t_f^2 + r^2} - \sqrt{t_i^2 + r^2}$. For $r \ll (t_i, t_f)$, $\tau(r) = \tau_0 \left(1 - r^2/2t_i t_f\right)$ whereas for $r \gg (t_i, t_f)$, $\tau(r) = \tau_0 \left(t_i + t_f\right)/2r$. In either case, the time interval decreases with increasing $r$, a result which can be read off of Fig. 2.

We have carried out a variety of numerical studies and found that generally the radiation of scalar waves is reasonably efficient. For example, in the simulations described above we find that most of the energy in the center of the two-bubble system is radiated away after only a few collisions. This result holds for a wide range of initial separations. We have also simulated the collision of two infinite plane walls in a theory with a symmetric double well potential (Eq.(2.2) with $\epsilon = 0$) and find that the percentage of energy radiated during a single collision is roughly constant and $\sim 30 - 40\%$ for a wide range ($0.3 < \gamma < 10$) of initial velocities (see, for example, Ref.[21]).

One can also consider first-order inflation in sine-Gordon (SG)-type theories. Here the potential is of the form

$$V = \lambda\phi_o^4 \left( \cos\left(\frac{\pi N \phi}{\phi_o}\right) + V_A(\phi) \right) \tag{4.5}$$

where there are $N$ local minima at $\phi = 2n\phi_o$ and $V_A$ creates a small asymmetry among these minima. For the most part, the dynamics of wall-wall interactions is determined by the first term in $V$. As is well known, SG kinks in a theory with $V_A = 0$ are true solitons, and infinite plane-symmetric walls pass through one another without dissipating any energy. However, if the walls are curved (or if $V_A \neq 0$) they will produce scalar radiation [22], though not as efficiently as $\phi^4$ walls. Reheating, in fact may be very different in these models (see also Section 5), though no detailed work has yet been done.

## 5. Particle Production

In order to reheat the Universe, the inflaton must couple to ordinary particles. This will allow the classical scalar waves described above to decay, eventually filling the Universe with a thermal bath at a temperature $T_{RH}$. These couplings also lead to direct production of particles during collisions between walls.

In this section we discuss this direct particle production. In particular, we consider production of fermions arising from interactions of the form $\mathcal{L}_1 = g_1 \phi \bar{\psi}\psi$ and $\mathcal{L}_2 = g_2 f^{-1} \bar{\psi}\gamma_\mu \psi \partial^\mu \phi$, where $f$ has units of mass. $\mathcal{L}_1$ is the typical Yukawa coupling of a scalar field to fermions. $\mathcal{L}_2$-type couplings arise if $\phi$ is a Goldstone (or pseudo-Goldstone) boson. In this case, the potential for $\phi$ is of the sine-Gordon (SG) type. As we will see, particle production in these two theories is dramatically different, though this is due as much to the peculiar properties of the SG walls as to the different form of the coupling between $\phi$ and $\psi$.

Our philosophy is to treat $\phi$ (the bubbles or walls) as a classical, external field and the fermions as quantum fields in the presence of this source (see, for example, Ref. [23]). In so doing we make no attempt to treat backreaction of particle production on the evolution of the walls.

The probability of producing at least one pair of particles is

$$P_{\geq 1} \;=\; 2\,\mathrm{Im}\,(\Gamma[\phi]) \tag{5.1}$$

where $\Gamma[\phi]$ is just the generating functional of one particle irreducible Green's functions:

$$\Gamma[\phi] \;=\; \sum_{n=2}^{\infty} \frac{1}{n!} \int d^4x_1 \cdots d^4x_n \Gamma^{(n)}\,(x_1,\ldots,x_n)\;\phi(x_1)\cdots\phi(x_n)\;. \tag{5.2}$$

$\Gamma[\phi]$ is also known as the effective action. In writing Eq.(5.1) we have assumed that $P_{\geq 1} \ll 1$.

To leading order

$$\Gamma[\phi] \;=\; \frac{1}{2}\int d^4x_1\; d^4x_2\;\phi(x_1)\;\phi(x_2)\;\Gamma^{(2)}\,(x_1,x_2) \tag{5.3}$$

or

$$\mathrm{Im}\,(\Gamma[\phi]) \;=\; \frac{1}{2}\int d^4x_1\; d^4x_2\;\phi(x_1)\;\phi(x_2)\int \frac{d^4p}{(2\pi)^4}\; e^{ip\cdot(x_1-x_2)}\;\mathrm{Im}\left(\tilde{\Gamma}^{(2)}(p^2)\right) \tag{5.4}$$

where $\tilde{\Gamma}^{(2)}(p^2)$ is the Fourier transform of $\Gamma^{(2)}\,(x_1,x_2)$. For either $\mathcal{L}_1$ or $\mathcal{L}_2$, the leading contribution to $\mathrm{Im}\left(\tilde{\Gamma}^{(2)}\right)$ comes in at the one-loop level. For $\mathcal{L}_1$ we find that

$$\mathrm{Im}\left(\tilde{\Gamma}^{(2)}(p^2)\right) = \frac{g_1^2 p^2}{8\pi}\left(1-\frac{4\mu^2}{p^2}\right)^{3/2}\Theta\left(p^2-4\mu^2\right) \tag{5.5}$$

where $\mu$ is the mass of $\psi$. Similarly, for $\mathcal{L}_2$ we have

$$\mathrm{Im}\left(\tilde{\Gamma}^{(2)}(p^2)\right) = \frac{g_2^2 p^4}{4\pi f^2}\left(1-\frac{4\mu^2}{p^2}\right)^{3/2}\Theta\left(p^2-4\mu^2\right)\;. \tag{5.6}$$

Let $\tilde{\phi}(p) \equiv \int d^4x\; e^{ip\cdot x}\phi(x)$ be the Fourier transform of $\phi$ We then have

$$\mathrm{Im}\,(\Gamma[\phi]) \;=\; \int \frac{d^4p}{(2\pi)^4}\;|\tilde{\phi}(p)|^2\;\mathrm{Im}\left(\tilde{\Gamma}^{(2)}(p^2)\right)\;. \tag{5.7}$$

This formula has a rather simple interpretation. The Fourier transform decomposes the scalar field into modes of definite four-momentum. Modes with $p^2 > 0$ represent propagating "particles" with mass $\mathcal{M}^2 = p^2$. (In general $\mathcal{M}^2 \neq m^2$, and these 'particles' are off-shell. However, they can still decay into on-shell fermions.) Eq.(5.7) sums over the number of particles with mass $\mathcal{M}$ contained in the field multiplied by the probability for those particles to decay. The $\theta$-function in Eq.(5.5) enforces the fact that only particles with $\mathcal{M} > 2\mu$ can decay.

As a first example, consider an infinite plane-symmetric domain wall. To keep things simple we assume a model with degenerate vacua so that a noninteracting wall will move with constant velocity. Since the result must be Lorentz-invariant, we can work in the rest frame of the wall. Clearly, in this frame $p_0 = 0$ for all modes, so that $p^2 < 0$ and there is no particle production.

Next, consider the head-on collision of two plane-symmetric walls. The walls can come from either $\phi^4$ or SG theories. As we will see, the crucial difference between the two models is that $\phi^4$ walls scatter off one another while SG walls pass through one another.

In principle, the calculation should be straightforward. One starts with the field configuration describing a collision. In the case of plane-symmetric walls moving in the $z$-direction, $\phi(\vec{x},t) = \phi(z,t)$. The next step is to calculate the Fourier transform. Here $\tilde{\phi}(\vec{k},\omega) = (2\pi)^2\delta(k_x)\delta(k_y)\tilde{\phi}(k_z,\omega)$. The final step is to substitute into Eq.(5.7) and integrate over $p$. This will give the number of particles produced per unit area:

$$\frac{N}{A} = 2\int \frac{dk\, d\omega}{(2\pi)^2} |\tilde{\phi}(k,\omega)|^2 \,\mathrm{Im}\left(\tilde{\Gamma}^{(2)}\left(\omega^2 - k^2\right)\right) \tag{5.8}$$

where $k \equiv k_z$.

The field configuration for colliding $\phi^4$-walls can be found numerically. However, the result will be quite complicated, as the scattering of two $\phi^4$ walls is inelastic. In general, scalar waves are produced in the collision whose decay will contribute to the particle production. It is difficult to untangle this contribution from that of the actual collision. We therefore choose to model the collision by treating the walls as infinitesimally thin and assuming that the scattering is perfectly elastic. This model should give accurate results for $k \ll \gamma m_\phi$ and $\omega \ll \gamma m_\phi / v$ in the case of relativistic walls.

Our ansatz for the field configuration is

$$\phi = \begin{cases} \phi_0, & \text{for } vt < z < -vt \text{ and } t < 0; \\ \phi_0, & \text{for } -vt < z < vt \text{ and } t > 0; \\ -\phi_0, & \text{otherwise} \end{cases} \tag{5.9}$$

and the Fourier transform of the field is

$$\tilde{\phi}(\vec{k},\omega) = \frac{8v\phi_0}{\omega^2 - k^2v^2}\ . \tag{5.10}$$

The slow power law-fall off at large $\omega^2 - k^2v^2$ is due to the fact that in our ansatz, $\phi$ is discontinuous. For realistic "thick" domain walls, $\tilde{\phi}$ would cut off exponentially for $k \gtrsim \gamma m_\phi$ and $\omega \gtrsim \gamma m_\phi / v$. Substituting Eqs.(5.5,5.10) into Eq.(5.7) we estimate

$$\frac{N}{A} \simeq g_1^2\phi_o^2 \ln\left(\frac{\gamma m_\phi}{2\mu}\right) \tag{5.11}$$

where we have assumed that $\gamma m_\phi \gg 2\mu$ and $\gamma \gg 1$. The energy per unit area radiated by the walls is

$$\frac{E}{A} \simeq g_1^2\phi_o^2\gamma m_\phi \tag{5.12}$$

which represents a fraction $g_1^2$ of the total energy in the walls in their center of mass frame.

As an ansatz for colliding, infinitely-thin SG walls, we take

$$\phi = \begin{cases} 0, & \text{for } vt < z < -vt\ ; \\ 2\phi_0, & \text{otherwise} \end{cases} \tag{5.13}$$

for $t < 0$ and

$$\phi = \begin{cases} 4\phi_0, & \text{for } vt < z < -vt\ ; \\ 2\phi_0, & \text{otherwise} \end{cases} \tag{5.14}$$

for $t > 0$. Here we assume a potential of the form Eq.(4.5)with $N = 1$ so that $\phi = \phi + 2\phi_0 n$. The Fourier transform of this field configuration is

$$\tilde{\phi}(k,\ \omega) = \frac{4\pi\phi_o}{ik}\ (\delta(\omega + kv) - \delta(\omega - kv))\ . \tag{5.15}$$

We see that $\tilde{\phi}$ is zero for $p^2 = \omega^2 - k^2 > 0$, implying that the number of particles produced is zero. Evidently, the particle production we have calculated in the $\phi^4$ case is due entirely to the fact that the walls reflect off of each other.

In the SG case it is easy to improve on this simplistic ansatz. In models with $V_A = 0$ there are exact analytical solutions for multi-soliton configurations. In particular, the field configuration for two domain walls traveling from $z = \pm\infty$ with velocities $\mp v$ is [24]

$$\phi_{SA}(z,t) = \frac{4\phi_o}{\pi}\tan^{-1}\left(\frac{v\cosh(\gamma m_\phi z)}{\sinh(\gamma v m_\phi t)}\right), \tag{5.16}$$

where $\gamma = 1/\sqrt{(1-v^2)}$ and the normalization is chosen to coincide with Eqs.(5.13,5.14) . The subscript 'SA' is borrowed from Ref.[24] and indicates that we are colliding a soliton and an antisoliton. We now calculate the Fourier transform of Eq.(5.16). The transform over $z$ can be done using an integration by parts and we find

$$\tilde{\phi}(k,t) = \frac{4\phi_o}{vk}\frac{\sin\left(\frac{kq}{2\gamma m_\phi}\right)\sinh(\gamma v m_\phi t)}{\sinh\left(\frac{q}{2}\right)\cosh\left(\frac{\pi k}{2\gamma m_\phi}\right)} \tag{5.17}$$

where $q = \cosh^{-1}\left(1 + 2v^{-2}\sinh^2(\gamma v m_\phi t)\right)$. We now assume that the walls are relativistic and expand in $1/\gamma$. Eq.(5.17) becomes

$$\tilde{\phi}(k,t) \simeq \frac{4\phi_o}{vk}\frac{1 - \frac{1}{2\gamma^2}}{\cosh\left(\frac{\pi k}{2\gamma m_\phi}\right)}\left(\sin(vkt) + \frac{k}{2\gamma^3 m_\phi}\cos(vkt)\tanh(\gamma v m_\phi t)\right)\ . \tag{5.18}$$

The first term corresponds to the result found in Eq.(5.15) and will not contribute to the particle production rate. For the second term we use the following transform:

$$\begin{aligned}\int_{-\infty}^{\infty} du\ e^{ibu}\cos au\tanh cu &= \int_0^{\infty} du\tanh cu\,(\sin(a+b)u + \sin(a-b)u) \\ &= \frac{\pi}{2c}\left(\sinh^{-1}\left(\frac{\pi(a+b)}{2c}\right) + \sinh^{-1}\left(\frac{\pi(a-b)}{2c}\right)\right)\ .\end{aligned} \tag{5.19}$$

The final result can be written in the form

$$\tilde{\phi}(\omega,k) \simeq \frac{4\pi\phi_o}{\gamma^4 m_\phi^2} \frac{\sinh\left(\frac{\pi\omega}{2\gamma v m_\phi}\right)}{\cosh\left(\frac{\pi\omega}{\gamma v m_\phi}\right) - \cosh\left(\frac{\pi k}{\gamma m_\phi}\right)} \ . \tag{5.20}$$

This result is similar in many respects to Eq.(5.10). For $\omega < \gamma v m_\phi$ and $k < \gamma m_\phi$, $\tilde{\phi} \propto \left(\omega^2 - v^2 k^2\right)^{-1}$. In addition $\tilde{\phi}$ is exponentially damped for larger values of $k$ and $\omega$, as anticipated above. We estimate that the number of particles produced per unit area is

$$\frac{N}{A} \simeq g_2^2 \phi_o^2 \left(\frac{m_\phi}{\gamma f}\right)^2 \tag{5.21}$$

and the energy lost per unit area is

$$\frac{E}{A} \simeq g_2^2 \phi_o^2 \gamma m_\phi \left(\frac{m_\phi}{\gamma f}\right)^2 \tag{5.22}$$

where again we have assumed that $\gamma m_\phi \gg 2\mu$. This represents a fraction $(g_2 m_\phi/\gamma f)^2$ of the total energy in the walls and is less than that found in the $\phi^4$ case by a factor $(m_\phi/f)^2\gamma^{-2}$. The $(m_\phi/f)^2$ term comes from the nature of the coupling $\mathcal{L}_2$ and is usually quite small.

Particle production in this case is due to a slight slowing down of the walls during their interaction. As $\gamma$ becomes large, the forces between the walls are able to effect a smaller change in velocity, leading to a smaller result for $N/A$. In principle, there will be similar effects in the $\phi^4$ case leading to corrections of order $1/\gamma^n$ to Eqs. (5.11) and (5.12).

Evidently, we can produce particles up to energy $\gamma m$. If the bubble walls are highly relativistic when they collide, there will be the possibility of producing particles well above the mass of the inflaton.

## 6. Conclusions

It is relatively easy to find a cosmological scenario which inflates. The challenge is in bringing an end to inflation so that the resultant universe resembles the one we live in. The vacuum energy which drives inflation must be converted into relativistic particles. Furthermore, fluctuations which arise during inflation should not lead to unacceptably large distortions in the microwave background. It is a bonus if they provide the seed perturbations necessary to drive the formation of large-scale structure. In addition, relics of the inflationary epoch such as gravity waves and topological defects may have survived until the present epoch. If detected these phenomena would provide a window to the very early Unverse.

The search for a truly graceful exit from inflation has had limited success. As is well known, most new and chaotic inflation scenarios require 'fine tuning' to satisfy the

microwave background constraints. Moreover, the spectrum of fluctuations arising in the simplest models appears to be inconsistent with observations of large-scale structure. In an attempt to overcome these difficulties, researchers have turned to alternative ways of implementing inflation. Extended and two-field inflation are two models arising from such a program. These theories invoke Guth's original idea that inflation proceed by a first order phase transition and have sparked a renewed interest in first-order inflation.

In this work, we begin to study the details reheating in first-order inflation. The ultimate goal of course is to predict, for a given model, the reheat temperature and spectrum of particles produced. Though we have not yet been reached this goal, we have developed the computational tools necessary to carry out such calculations. In particular, we have studied the expansion and collisions of bubbles as well as particle production from quantum effects.

Our results indicate that energy in bubble walls is efficiently converted into scalar radiation when the walls collide, suggesting that reheating in these models is not all that different from reheating in new and chaotic inflation. However, caution should be used in applying this result to all models. As noted in Section 2, there are four parameters describing a first-order inflation model ($\Delta$, $R_o$, $D$, and $H$ or $\lambda$, $\epsilon$, $\eta$, and $m_{pl}$) some or all of which vary in time during both inflation and reheating. There may indeed be regimes of parameter space in which energy stays in walls for a fairly long period of time. Furthermore, walls in sine-Gordon type theories are far less dissipative. In these theories, energy might remain in coherent scalar field configurations for many Hubble times leading to a lower reheat temperature.

Finally, we have studied particle production during wall collisions. We find that the results differ markedly depending on whether the walls pass through each other or are reflected, but are otherwise independent of the details of the model considered. We note that this work may have applications to particle production from scalar field configurations in other contexts such as late-time phase transitions.

First order inflation theories have a potentially rich phenomenology. The key is to find some observable consequence which will determine whether or not a first order inflationary phase transition occured in the early Universe. We hope that this work will aid in these investigations.

## Acknowledgements

We thank S. Dodelson, H. Feldman, J. Frieman, B. Greene, L. Kofman, E. W. Kolb, M. Merrifield, and A. Stebbins for useful discussions. This work began during the 1990 Summer session at the Aspen Center for Physics and we thank the Center for hospitality during our stay. This work was supported in part by the NASA (NAGW-1340 at Fermilab) and by the DOE (at Chicago and Fermilab).

## Figure Captions

1. Spacetime diagram for a two bubble collision. The diagram gives the field configuration in the $s' - z$ plane ($t > \sqrt{x^2 + y^2}$). The nucleation sites are at the bottom righthand and bottom lefthand corners of the digram. The false vacuum is shown in

black, the true vacuum in light gray. Regions where $\phi < -\phi_o$ appear white. In Fig. 1b the initial separation beteen the bubbles has been doubled and the coordinates have been scaled by a factor 1/2.

2. Spacetime diagram in the $t - r$ plane for the two-bubble collision shown in Fig. 1a. For this diagram, $z = 0$.
3. Field configuration shown at different times during the collision. Note the scalar radiation emanating from the collision region.
4. Spacetime diagrams illustrating a big bubble hitting a small bubble. Fig. 4a shows the two-bubble collision in the equal bubble (simultaneous-nucleation) frame. Here, the radiation is symmetric about $z = 0$. Fig. 4b shows the same configuration in a Lorentz-boosted frame. The bubble on the left is nucleated first and is larger at the time of the collision. In this frame, all of the radiation is moving to the right, away from the nucleation site of the big bubble.

## References


[1] A. H. Guth, *Phys. Rev. D* **23** (1981) 347.

[2] A. H. Guth and E. J. Weinberg, *Nucl. Phys.* **B212** (1983) 321.

[3] D. La and P. J. Steinhardt, *Phys. Rev. Lett.* **62** (1989) 376.

[4] E. J. Weinberg, *Phys. Rev. D* **40** (1989) 3950.

[5] P. J. Steinhardt and F. S. Accetta, *Phys. Rev. Lett.* **64** (1990) 123; F. Adams and K. Freese, *Phys. Rev. D* **43** (1991) 353; A. D.Linde, *Phys. Lett.* **B249** (1990) 18; R. Holman, E. W. Kolb, and Y.Wang, *Phys. Rev. Lett.* **65** (1990) 17.

[6] A. D. Linde, *Phys. Lett.* **129B** (1983) 177; A. Albrecht and P. J. Steinhardt, *Phys. Rev. Lett.* **48** (1982) 1220.

[7] A. D. Linde, *Phys. Lett.* **129B** (1983) 177.

[8] A. Albrecht, P. J. Steinhardt, M. S. Turner, and F. Wilczek, *Phys. Rev. Lett.* **48** (1982) 1437; L. Abbott, E. Farhi, and M. Wise, *Phys. Lett.* **117B** (1982) 29; A. Dolgov and A. D. Linde, *Phys. Lett.* **116B** (1982) 329.

[9] M. S. Turner and F. Wilczek, *Phys. Rev. Lett.* **65** (1990) 3080.

[10] S. W. Hawking, I. G. Moss, and J. M. Stewart, *Phys. Rev. D* **26** (1982) 2681.

[11] J. D. Barrow, E. J. Copeland, E. W. Kolb, and A. R. Liddle, *Phys. Rev. D* **43** (1991) 984.

[12] E. J. Copeland, E. W. Kolb, and A. R. Liddle, *Phys. Rev. D* **42** (1990) 2911.

[13] J. D. Barrow, E. J. Copeland, E. W. Kolb, and A. R. Liddle, *Phys. Rev. D* **43** (1991) 977.

[14] S. Coleman, *Phys. Rev. D* **16** (1977) 1762.

[15] S. Colman, V. Glaser, and A. Martin, *Comm. Math. Phys.* **58** (1978) 211.

[16] S. Coleman and F. De Luccia, *Phys. Rev. D* **21** (1980) 3305.

[17] C. G. Callan and S. Coleman, *Phys. Rev. D* **16** (1977) 1762.

[18] G. B. Gelmini, M. Gleiser, and E. W. Kolb, *Phys. Rev. D* **39** (1989) 1558.

[19] W. Israel, *Nuovo Cimento* **44B** (1966) 1. See, also J. Ipser and P. Sikivie, *Phys. Rev. D* **30** (1984) 712.

[20] D. Seckel, in *Inner Space: Outer Space*, eds. E. W. Kolb, et al. (The University of Chicago Press, Chicago, 1986).

[21] T. I. Belova and A. E. Kudryavtsev, *Physica* **D32** (1988) 18 and references therein.

[22] L. M. Widrow, *Phys. Rev. D* **40** (1989) 1002.

[23] C. Itzykson and J. Zuber, *Quantum Field Theory*, (McGraw-Hill Inc, 1980).

[24] G. Bowtell and A. E. G. Stuart, *Phys. Rev. D* **15** (1977) 3580.

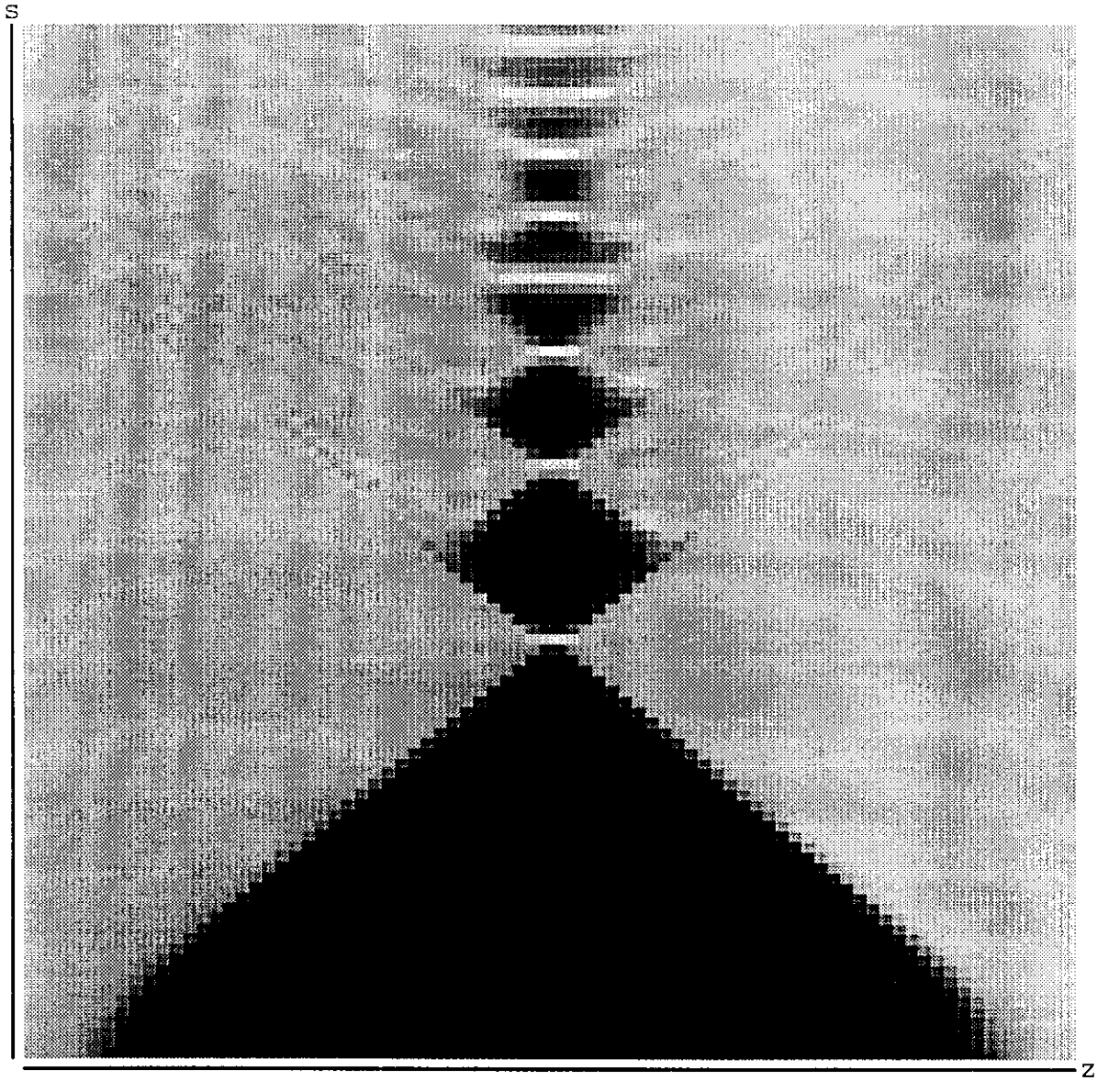


- FIG 1a -

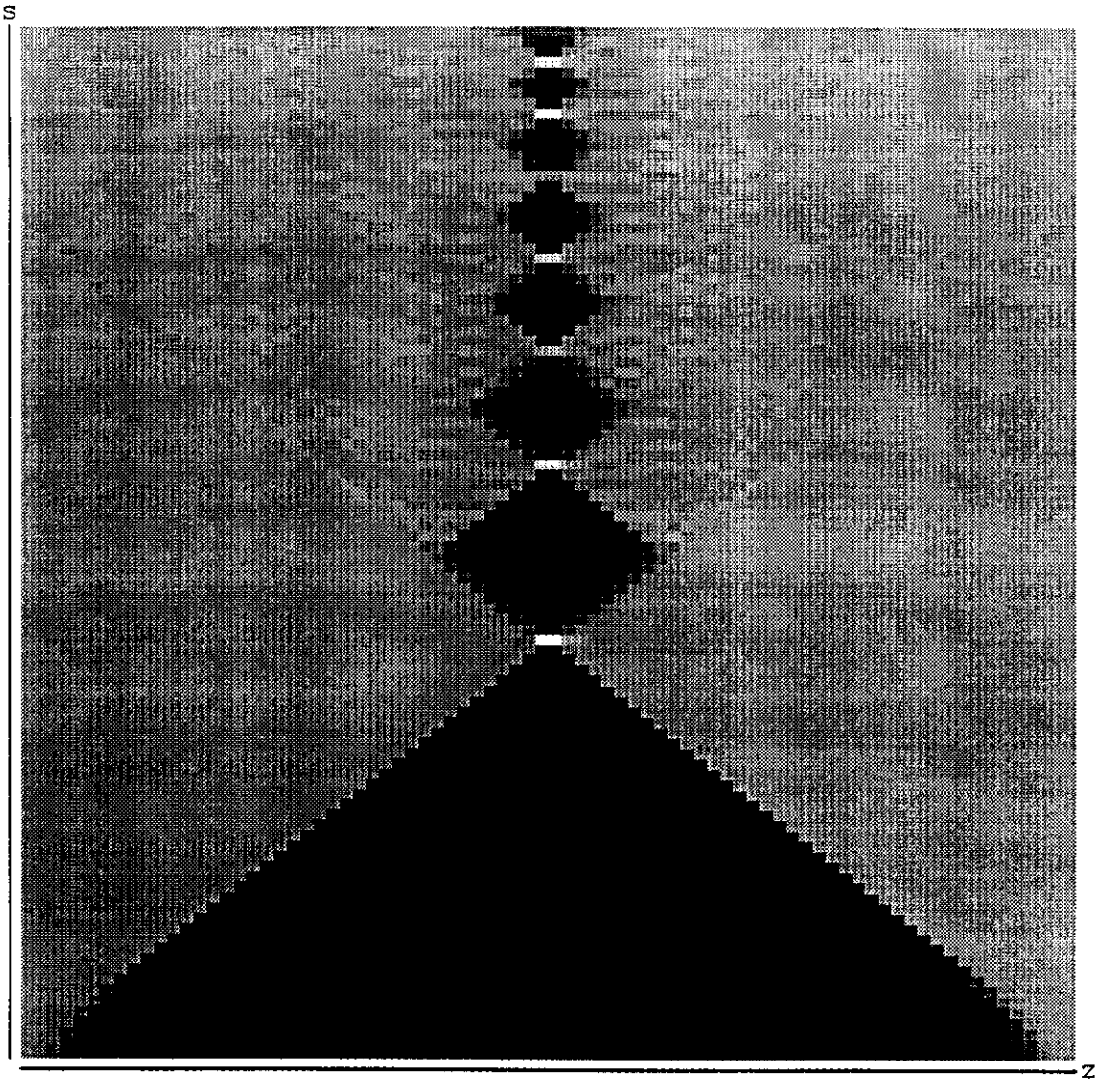


- FIG 16 -

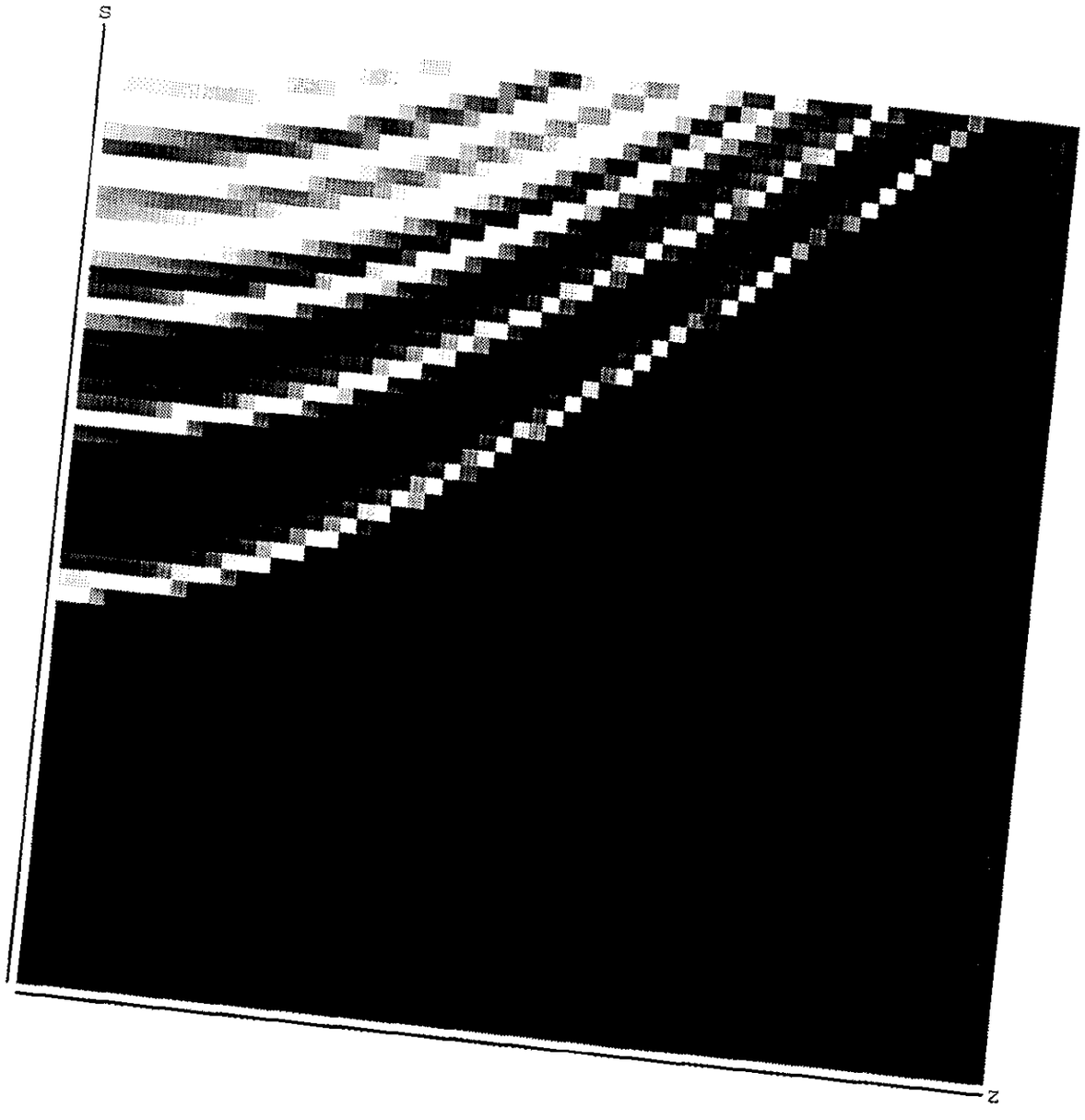


- FIG 2 -

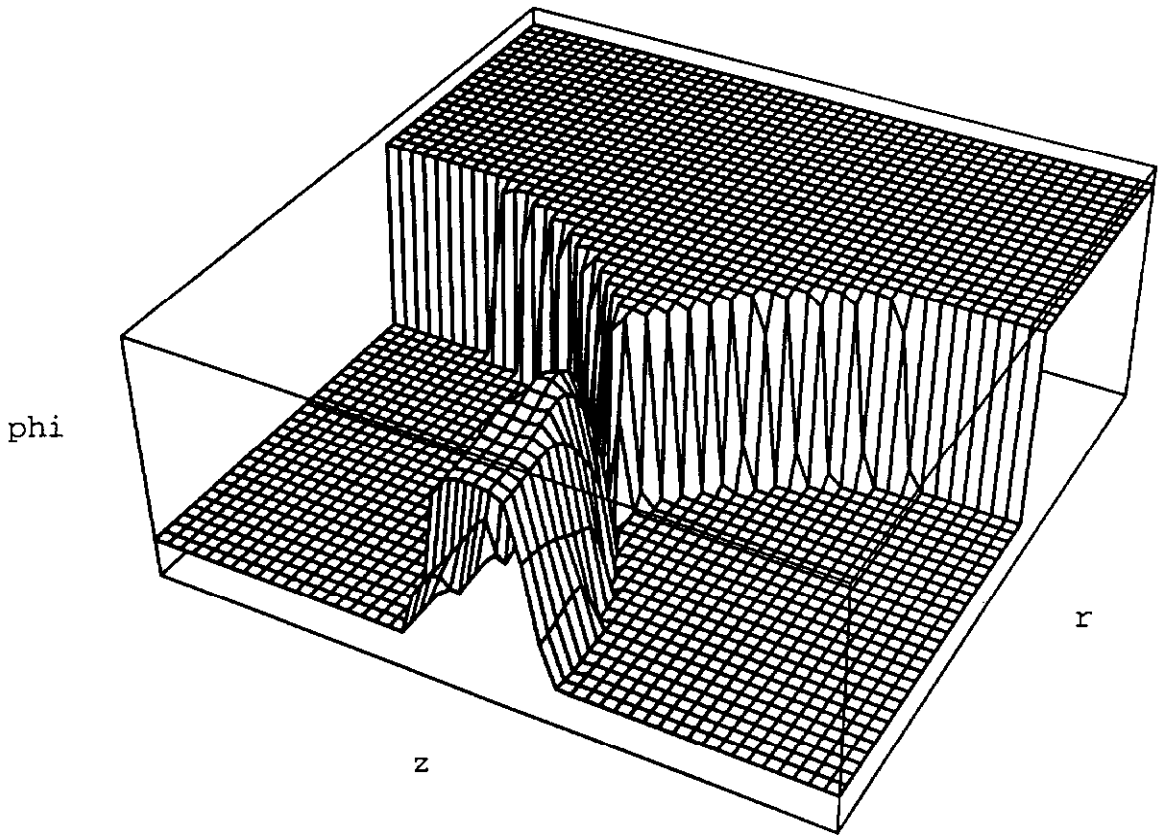


– FIG 3a –

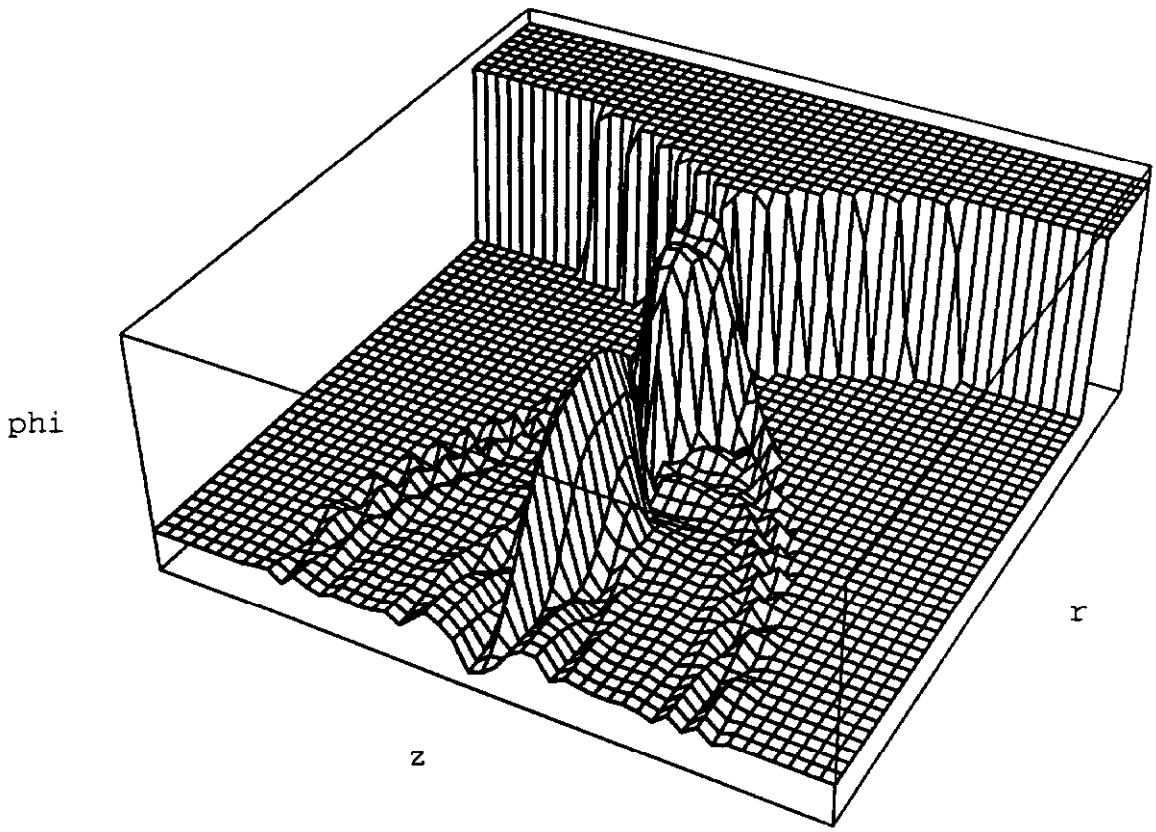


- FIG 3b -

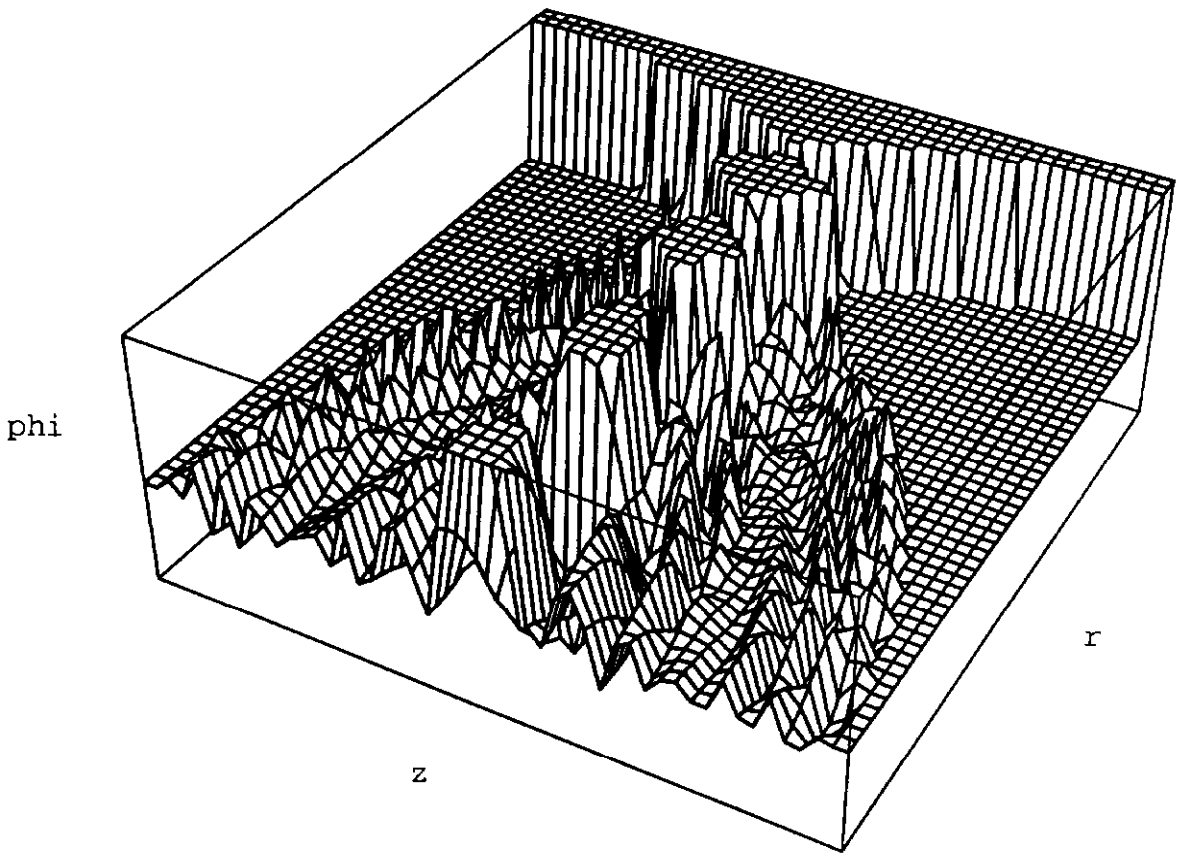


— FIG. 3C —

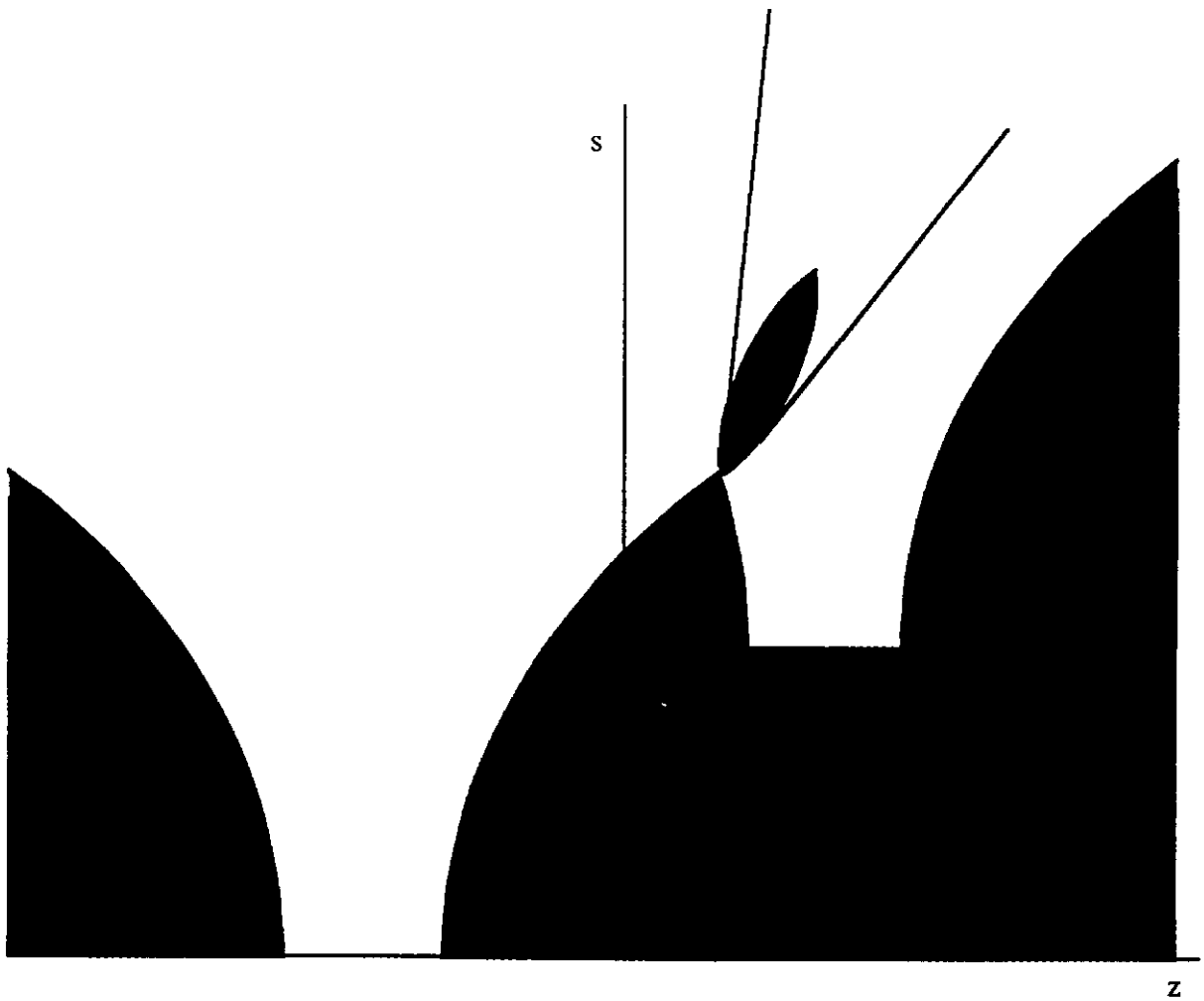


— FIG 4b —

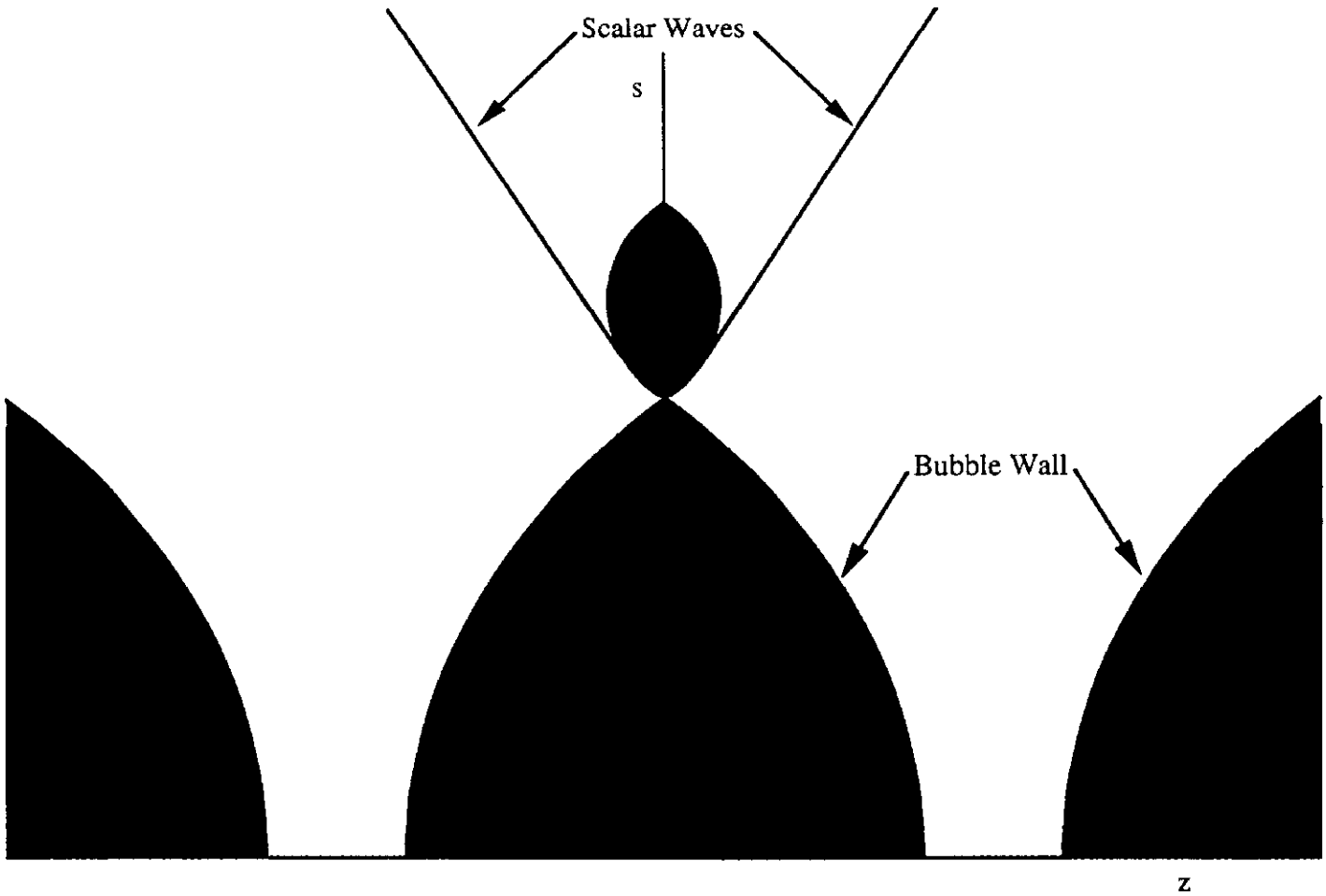


— FIG 4a —